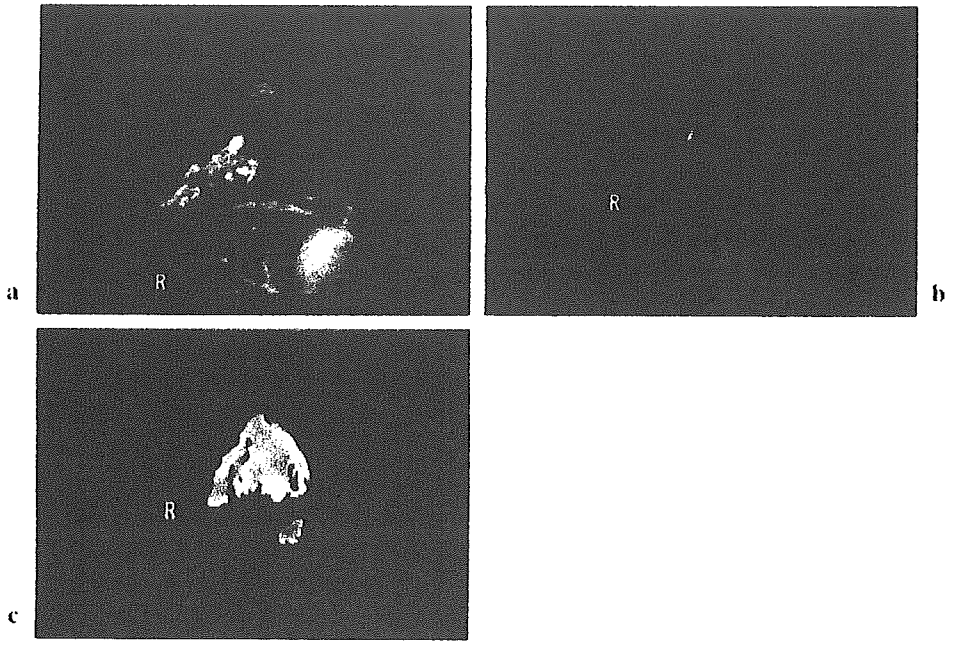

Fig. 3. A case of ductal carcinoma *in situ*
a: Maximum intensity projection (MIP) image of subtraction image obtained with 3DFSPGR. The segmental nodular enhancement is displayed in area C.
b: DWI in the axial plane shows a segmental high-intensity lesion in area C.
c: An ADC map of the same level as Fig. 3b. The greenish color indicates a low ADC value. The distribution of low ADC values corresponds to the enhancement lesion of MIP image on Fig. 3a.

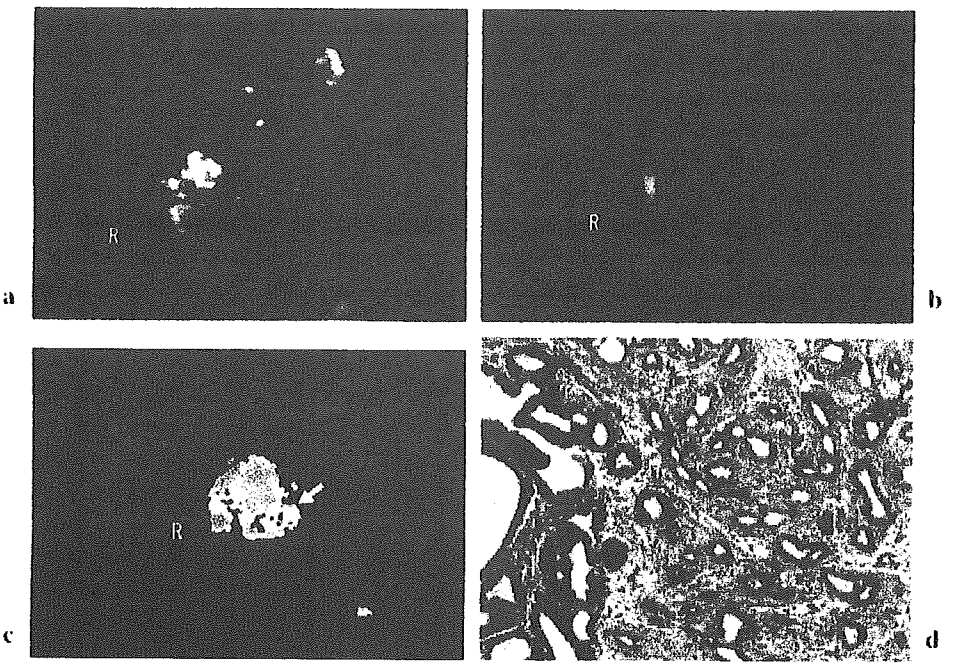

Fig. 4. A case of scirrhous carcinoma
a: MIP of subtraction image obtained with 3DFSPGR. The enhanced mass lesion in area C indicates a primary mass lesion. Note the diffuse scattering of small enhanced nodules in the mammary gland.
b: DWI reveals a high-intensity lesion in area C as a 3DFSPGR image.
c: An ADC map of the same level as Fig. 4b. The primary mass lesion shows a low ADC value. Area A also shows a low ADC region (white arrow).
d: Pathologic figure of area A. The sclerosing adenosis is prominent (H&E, ×40).

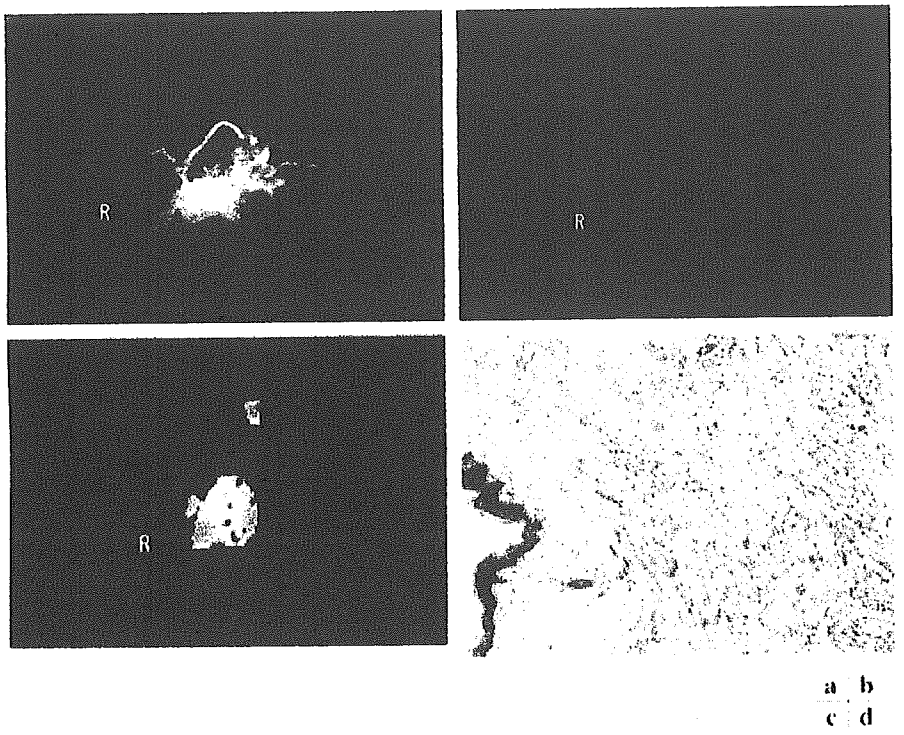

Fig. 5. A case of invasive lobular carcinoma
a: A MIP image of a subtraction image shows a speculated enhanced mass lesion extending from area A to area C. Some linear and nodular enhancements extend to the nipple site, which suggest tumor invasion.
b: DWI reveals a localized high-intensity lesion in area C that is smaller than the enhanced lesion in the 3DFSPGR image.
c: A low ADC area is evident in area C. The extending enhanced lesion obtained with 3DFSPGR is not visualized on the ADC map.
d: Histologic appearance of the area where the 3DFSPGR image shows enhancement, whereas the ADC map did not show ADC reduction (H&E, ×100). Sparse and scattered distribution of cancer cells is evident in the stroma.

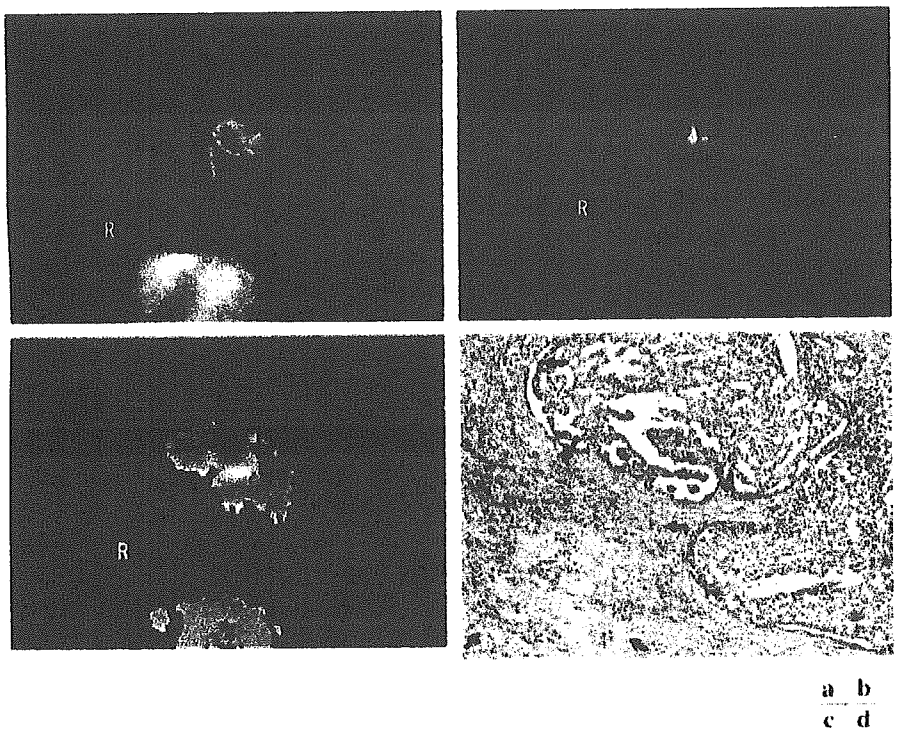

Fig. 6. A case of intracystic papillary carcinoma surrounded by intraductal carcinoma
a: A cystic mass lesion in area D. The irregular mass along the wall of the cystic mass protrudes inward. Some nodular enhancement is evident around the cystic mass lesion.
b: DWI of the same level as that of Fig. 5a. The high-intensity lesion of DWI corresponds approximately to the 3DFSPGR image.
c: ADC map of the same level as that of Fig. 5b. The low ADC area is absent.
d: The histopathologic figure neighboring the lesion of intracystic papillary carcinoma shows hemosiderine-laden macrophage surrounding the intraductal carcinoma component (black arrow; H&E, ×40).

cell density, tumor structure, intestinal structure, and tissue components such as edema, necrosis, and fibrosis. With regard to breast DWI, a high sensitivity to breast malignant tumor has been already proven. Y. Guo demonstrated 93% sensitivity with the threshold of 1.3×10^{-3} mm^2/s of ADC value for breast cancer, while Y. Kuroki et al. showed statistically lower ADC values for breast carcinomas than those of benign tumors.[3,15] Our study showed a 93% sensitivity to malignant tumors among the G-1, G-2, and G-3 cases, with a threshold of 1.6×10^{-3} mm^2/s of ADC value. As

for the false negative cases and underestimated cases, in which the ADC values were not decreased in the carcinoma components, notable histopathologic characteristics were observed in the specimens, specifically necrosis and hemorrhage. Seven cases of G-3 and 9 cases of G-4 showed hemorrhage or necrosis mainly owing to DCIS or malignant phyllodes tumor. Conversely, hemorrhage was also observed in some specimens of intraductal papilloma. However, most intraductal papilloma showed low ADC values. The reason for this anomaly is unknown. We speculate that the character of the hemorrhage differs between the malignant tumors and intraductal papilloma. Comedo-type DCIS show the phenomenon of necrosis, hemorrhage, and calcification. We hypothesize that the high degree of oxidation as a consequence of necrosis affects the high ADC value. Specifically, the strong effect of magnetic susceptibility is one mechanism of high ADC values in DCIS and malignant phyllodes tumor with bleeding. Since seven of the bleeding cases showed high intensity in T_1-weighted images, it is possible to speculate about the occurrence of hemorrhage by referring to other sequences.

In 3 cases categorized as G-3, scattering and sparse distribution of lobular carcinoma and DCIS did not represent low ADC values. Moreover, with respect to 11 cases categorized as G-1 in which the ADC map did not show low values in DCIS around main tumors, one reason for the misdiagnosis is the limited spatial resolution of DWI. However, the sensitivity to small foci and the sparse distribution of tumor will improve with advances in the spatial resolution of DWI.

As for benign lesions, although Guo et al. showed all fibroadenoma were correctly diagnosed as benign lesions, one case of duct ectasia and one of intraductal papilloma were incorrectly categorized.[3] In our study, specificity was markedly low. Most cases of intraductal papilloma and more than half the cases of fibrocystic disease showed low ADC values and were categorized as malignant lesions. Moreover, benign proliferative changes such as ductal hyperplasia, fibroadenosis, and lobular hyperplasia around the carcinoma have resulted in over-estimation of cancer extension. Some pathogenesis of this phenomenon can be considered. Guo et al. confirmed the relation between ADC values and cell density, which exhibited an inverse proportion. Fibrocystic disease sometimes shows a high cell density and inflammatory reactions. This phenomenon restricts proton diffusion, a possible reason for low ADC values. However, the disparity between the ADC values of fibrocystic disease and malignancy could be divided further with a higher b-value. This is because the effect of perfusion is smaller at higher b-values and the reduction in ADC values of malignant lesions is more prominent than that of benign lesions due to angiogenesis of malignant tumor.[16,30] Only two cases of fibroadenoma were found in our study, both of the pericanalicular type, and both exhibited low ADC values. Although Guo et al. did not mention the detailed type of fibroadenoma, it is possible that not all fibroadenoma will show high ADC values. Therefore, ADC values are still unreliable for fibrocystic disease, intraductal papilloma, and some types of fibroadenoma. As our study showed low specificity, DWI is still insufficient for qualitative diagnosis.

Conclusion

Our trial sought to verify the usefulness of breast DWI in clinical applications. We discovered that the sensitivity is sufficient for detecting malignant lesions. In addition, with DWI we were able to obtain images with one-minute scan times. This satisfies the requirements for screening use. This study demonstrated the potential for DWI to be used in the assessment of cancer extension. The spatial resolution and accuracy of differentiation will be improved with advances in MRI technology.

References

1. Filippi M, Cercignani M, Inglese M, et al. Diffusion tensor magnetic resonance imaging in multiple sclerosis. Neurology 2001; 56:304–311.
2. Bammer R. Basic principles of diffusion-weighted imaging. Eur J Radiol 2002; 45:169–184.
3. Guo Y, Cai YQ, Cai ZL, et al. Differentiation of clinically benign and malignant breast lesions using diffusion-weighted imaging. J Magn Reson Imaging 2002; 16:172–178.
4. Lyng H, Haraldseth O, Rofsrad EK. Mesurement of cell density and necrotic fraction in human melanoma xenografts by diffusion weighted magnetic resonance imaging. Magn Reson Med 2000; 43:828–836.
5. Warach S, Boska M, Welch KM. Pitfalls and potential of clinical diffusion-weighted MR imaging in acute stroke. Stroke 1997; 28:481–482.
6. Noguchi K, Watanabe N, Nagayoshi T, et al. Role of diffusion-weighted echo planar MRI in distinguishing between brain abscess and tumour: a preliminary report. Neuroradiology 1999; 41:171–174.
7. Tsuruda JS, Chew WM, Moseley ME, et al. Diffusion-weighted MR imaging of the brain: value of differentiating between extraaxial cysts and

epidermoid tumors. AJNR Am J Neuroradiol 1990; 11:925-931.
8. Kim T, Murakami T, Takahashi S, et al. Diffusion weighter single-shot echoplanar MR imaging for liver disease. AJR Am J Roentgenol 1999; 173: 393-398.
9. Namimoto T, Yamashita Y, Sumi S, et al. Focal liver masses: characterization with diffusion-weighted echo planar MR imaging. Radiology 1997; 04:739-744.
10. Kuroki S, Nasu S, Murakami K, et al. Pancreatic cancer on DWI. Nippon Acta Radiol 2003; 63: S184.
11. Moteki T, Ishizaka H, Horikoshi H, et al. Differentiation between hemangiomas and hepatocellular carcinomas with the apparent diffusion coefficient calculated from turboFLASH MR images. JMR 1995; 5:187-191.
12. Moteki T. Ishizaka H. Diffusion-weighted EPI of cystic ovarian lesions: evaluation of cystic contents using apparent diffusion coefficients. J Magn Reson Imaging 2000: 12:1014-1019.
13. Maier CF, Paran Y, Bendel P, et al. Quantitative diffusion imaging in implanted human breast tumors. Magn Reson Med 1997; 37:576-581.
14. Englander SA, Ulug AM, Brem R, et al. Diffusion imaging of human breast. NMR Biomed 1997; 10:348-352.
15. Kuroki Y, Katsushiro N, Kuroki S, et al. Diffusion-weighted imaging of breast cancer with the sensitivity encoding technique: analysis of apparent diffusion coefficient value. MRMS 2004; 3:79-85.
16. Buadu LD, Murakami J, Murayama S, et al. Breast lesions: correlation of contrast medium enhancement patterns on MR images with histopathologic findings and tumor angiogenesis. Radiology 1996; 200:639-649.
17. Mumtaz H, Hall-Craggs MA, Davidson T, et al. Staging of symptomatic primary breast cancer with MR imaging. AJR Am J Roentgenol 1997; 169: 417-424.
18. Morris EA, Schwartz LH, Dershaw DD, et al. MR imaging of the breast in patients with occult primary breast carcinoma. Radiology 1997; 205:437-440.
19. Boné B, Péntek Z, Perbeck L, et al. Diagnostic accuracy of mammography and contrast-enhanced MR imaging in 238 histologically verified breast lesions. Acta Radiol 1997; 38:489-496.
20. Stomper PC, Winston JS, Herman S, et al. Angiogenesis and dynamic MR imaging gadolinium enhancement of malignant and benign breast lesions. Breast Cancer Res Treat 1997; 45:39-46.
21. Boetes C, Barentsz JO, Mus RD, et al. MR characterization of suspicious breast lesions with a gadolinium-enhanced turbo FLASH subtraction technique. Radiology 1994; 193:777-781.
22. Heiberg EV, Perman WH, Herrmann VM, et al. Dynamic sequential 3D gadolinium-enhanced MRI of the whole breast. Magn Reson Imaging 1996; 14:337-348.
23. Baum F, Fischer U, Vosshenrich R, et al. Classification of hypervascularized lesions in CE MR imaging of the breast. Eur Radiol 2002; 12:1087-1092.
24. Fischer U, Kopka L, Grabbe E. Breast carcinoma: effect of preoperative contrast-enhanced MR imaging on the therapeutic approach. Radiology 1999; 13:881-888.
25. Orel SG, Schnall MD, Powell CM, et al. Staging of suspected breast cancer: effect of MR imaging and MR-guided biopsy. Radiology 1995; 196:115-122.
26. Rieber A, Merkle E, Böhm W, Brambs H-J, Tomczak R. MRI of histologically confirmed mammary carcinoma: clinical relevance of diagnostic procedures for detection of multifocal or contralateral secondary carcinoma. J Comput Assist Tomogr 1997; 21:773-779.
27. Boetes C. Strijk SP. Holland R. et al. False-negative MR imaging of malignant breast tumors. Eur Radiol 1997; 7:1231-1234.
28. Cohen EK, Leonhardt CM, Shumak RS, et al. Magnetic resonance imaging in potential postsurgical recurrence of breast cancer: pitfalls and limitations. Can Assoc Radiol J 1996; 47:171-176.
29. Liu PF. Debatin JF. Caduff RF, et al. Improved diagnostic accuracy in dynamic contrast enhanced MRI of the breast by combined quantitative and qualitative analysis. Br J Radiol 1998; 71:501-509.
30. Hulka CA, Smith BL, Sgroi DC, et al. Benign and malignant breast lesions: differentiation with echoplanar MR imaging. Radiology 1995; 197:33-38.

VOLUME 23 · NUMBER 6 · FEBRUARY 20 2005

JOURNAL OF CLINICAL ONCOLOGY

ORIGINAL REPORT

Randomized Pharmacokinetic and Pharmacodynamic Study of Docetaxel: Dosing Based on Body-Surface Area Compared With Individualized Dosing Based on Cytochrome P450 Activity Estimated Using a Urinary Metabolite of Exogenous Cortisol

Noboru Yamamoto, Tomohide Tamura, Haruyasu Murakami, Tatsu Shimoyama, Hiroshi Nokihara, Yutaka Ueda, Ikuo Sekine, Hideo Kunitoh, Yuichiro Ohe, Tetsuro Kodama, Mikiko Shimizu, Kazuto Nishio, Naoki Ishizuka, and Nagahiro Saijo

From the Division of Internal Medicine, National Cancer Center Hospital; Pharmacology Division and Cancer Information and Epidemiology Division, National Cancer Center Research Institute, Tokyo, Japan.

Submitted November 7, 2003; accepted August 19, 2004.

Supported in part by a Grant-in-Aid for Cancer Research (9-25) from the Ministry of Health, Labor, and Welfare, Tokyo, Japan.

Presented in part at the 38th Annual Meeting of the American Society of Clinical Oncology, May 18-21, 2002, Orlando, FL.

Authors' disclosures of potential conflicts of interest are found at the end of this article.

Address reprint requests to Tomohide Tamura, MD, Division of Internal Medicine, National Cancer Center Hospital, 5-1-1, Tsukiji, Chuo-ku, Tokyo, 104-0045, Japan; e-mail: ttamura@ncc.go.jp.

0732-183X/05/2306-1061/$20.00

DOI: 10.1200/JCO.2005.11.036

ABSTRACT

Purpose

Docetaxel is metabolized by cytochrome P450 (CYP3A4) enzyme, and the area under the concentration-time curve (AUC) is correlated with neutropenia. We developed a novel method for estimating the interpatient variability of CYP3A4 activity by the urinary metabolite of exogenous cortisol (6-beta-hydroxycortisol [6-β-OHF]). This study was designed to assess whether the application of our method to individualized dosing could decrease pharmacokinetic (PK) and pharmacodynamic (PD) variability compared with body-surface area (BSA) –based dosing.

Patients and Methods

Fifty-nine patients with advanced non–small-cell lung cancer were randomly assigned to either the BSA-based arm or individualized arm. In the BSA-based arm, 60 mg/m^2 of docetaxel was administered. In the individualized arm, individualized doses of docetaxel were calculated from the estimated clearance (estimated clearance = 31.177 + [7.655 × 10^{-4} × total 6-β-OHF] − [4.02 × alpha-1 acid glycoprotein] − [0.172 × AST] − [0.125 × age]) and the target AUC of 2.66 mg/L · h.

Results

In the individualized arm, individualized doses of docetaxel ranged from 37.4 to 76.4 mg/m^2 (mean, 58.1 mg/m^2). The mean AUC and standard deviation (SD) were 2.71 (range, 2.02 to 3.40 mg/L · h) and 0.40 mg/L · h in the BSA-based arm, and 2.64 (range, 2.15 to 3.07 mg/L · h) and 0.22 mg/L · h in the individualized arm, respectively. The SD of the AUC was significantly smaller in the individualized arm than in the BSA-based arm ($P < .01$). The percentage decrease in absolute neutrophil count (ANC) averaged 87.1% (range, 59.0 to 97.7%; SD, 8.7) in the BSA-based arm, and 87.4% (range, 78.0 to 97.2%; SD, 6.1) in the individualized arm, suggesting that the interpatient variability in percent decrease in ANC was slightly smaller in the individualized arm.

Conclusion

The individualized dosing method based on the total amount of urinary 6-β-OHF after cortisol administration can decrease PK variability of docetaxel.

J Clin Oncol 23:1061-1069. © 2005 by American Society of Clinical Oncology

INTRODUCTION

Many cytotoxic drugs have narrow therapeutic windows despite having a large interpatient pharmacokinetic (PK) variability. The doses of these cytotoxic drugs are usually calculated on the basis of body-surface area (BSA). Although several physiologic functions are proportional to BSA, systemic exposure to a drug is only partially related to

this parameter.[1-3] Consequently, a large interpatient PK variability is seen when doses are based on BSA. This large interpatient PK variability can result in undertreatment with inappropriate therapeutic effects in some patients, or in overtreatment with unacceptable severe toxicities in others. Understanding interpatient PK variability is important for optimizing anticancer treatments. Factors that affect PK variability include drug absorption, metabolism, and excretion. Among these factors, drug metabolism is regarded as a major factor causing PK variability. Unfortunately, however, no simple and practical method for estimating the interpatient variability of drug metabolism is available. If drug metabolism in each patient could be predicted, individualized dosing could be performed to optimize drug exposure while minimizing unacceptable toxicity.

Docetaxel is a cytotoxic agent that promotes microtubule assembly and inhibits depolymerization to free tubulin, resulting in the blockage of the M phase of the cell cycle.[4] Docetaxel has shown promising activity against several malignancies, including non–small-cell lung cancer, and is metabolized by hepatic CYP3A4 enzyme.[5-15]

Human CYP3A4 is a major cytochrome P450 enzyme that is present abundantly in human liver microsomes and is involved in the metabolism of a large number of drugs, including anticancer drugs.[16-18] This enzyme exhibits a remarkable interpatient variation in activity as high as 20-fold, which accounts for the large interpatient differences in the disposition of drugs that are metabolized by this enzyme.[19-22] Several noninvasive in vivo probes for estimating the interpatient variability of CYP3A4 activity have been reported and include the erythromycin breath test, the urinary dapsone recovery test, measurement of midazolam clearance (CL), and measurement of the ratio of endogenous urinary 6-beta-hydroxycortisol (6-β-OHF) to free-cortisol (FC).[23-27] The erythromycin breath test and the measurement of midazolam CL are the best validated, and both have been shown to predict docetaxel CL in patients.[28,29] However, neither probe has been used in a prospective study to validate the correlations observed, or to test their utility in guiding individualized dosing.

We developed a novel method for estimating the interpatient variability of CYP3A4 activity by urinary metabolite of exogenous cortisol. The total amount of 24-hour urinary 6-β-OHF after cortisol administration (total 6-β-OHF) is significantly correlated with docetaxel CL, which is metabolized by the CYP3A4 enzyme. We also illustrate the possibility that individualized dosing to optimize drug exposure and decrease interpatient PK variability could be performed using this method.[30]

We conducted a prospective, randomized PK and pharmacodynamic (PD) study of docetaxel comparing BSA-based dosing and individualized dosing based on the interpatient variability of CYP3A4 activity, as estimated by a urinary metabolite of exogenous cortisol. The objective of this study was to assess whether the application of our method to individualized dosing could decrease PK and PD variability of docetaxel compared with BSA-based dosing.

PATIENTS AND METHODS

Patient Selection

Patients with histologically or cytologically documented advanced or metastatic non–small-cell lung cancer were eligible for this study. Other eligibility criteria included the following: age $\geq$ 20 years; Eastern Cooperative Oncology Group performance status of 0, 1, or 2; 4 weeks of rest since any previous anticancer therapy; and adequate bone marrow (absolute neutrophil count [ANC] $\geq$ 2,000/μL and platelet count $\geq$ 100,000/μL), renal (serum creatinine level $\leq$ 1.5 mg/dL), and hepatic (serum total bilirubin level $\leq$ 1.5 mg/dL, AST level $\leq$ 150 U/L, and ALT level $\leq$ 150 U/L) function. Written informed consent was obtained from all patients before enrollment onto the study.

The exclusion criteria included the following: pregnancy or lactation; concomitant radiotherapy for primary or metastatic sites; concomitant chemotherapy with any other anticancer agents; treatment with steroids or any other drugs known to induce or inhibit CYP3A4 enzyme[17]; serious pre-existing medical conditions, such as uncontrolled infections, severe heart disease, diabetes, or pleural or pericardial effusions requiring drainage; and a known history of hypersensitivity to polysorbate 80. This study was approved by the institutional review board of the National Cancer Center.

Pretreatment and Follow-Up Evaluation

On enrollment onto the study, a history and physical examination were performed, and a complete differential blood cell count (including WBC count, ANC, hemoglobin, and platelets), and a clinical chemistry analysis (including serum total protein, albumin [ALB], bilirubin, creatinine, AST, ALT, gamma-glutamyltransferase, alkaline phosphatase [ALP], and alpha-1 acid glycoprotein [AAG]) were performed. Blood cell counts and a chemistry analysis except for AAG were performed at least twice a week throughout the study. Tumor measurements were performed every two cycles, and antitumor response was assessed by WHO standard response criteria. Toxicity was evaluated according to the National Cancer Institute Common Toxicity Criteria (version 2.0).

Study Design

This study was designed to assess whether the application of our method to individualized dosing could decrease PK and PD variability compared with BSA-based dosing. The primary end point was PK variability and the secondary end point was PD variability (ie, toxicity). In our previous study involving 29 patients who received 60 mg/m^2 of docetaxel, the area under the concentration-time curve (AUC) was calculated to be 2.66 $\pm$ 0.91 (mean $\pm$ standard deviation [SD]) mg/L $\cdot$ h.[30] We assumed that the variability of AUC, represented by the SD, could be reduced by 50% in the individualized arm compared with that in the BSA-based arm, and that AUC would be normally distributed. The required sample size was 25 patients per arm to detect this difference with a two-sided F test at α = .05 and a power of 0.914.

Patients were randomly assigned to either the BSA-based arm or individualized arm (Fig 1). In the BSA-based arm, each patient received a dose of 60 mg/m^2 of docetaxel. In the individualized arm, individualized doses of docetaxel were calculated from the estimated docetaxel CL after cortisol administration and the target AUC (described in the Docetaxel Administration section).

Cortisol Administration and Urine Collection

In the individualized arm, 300 mg of hydrocortisone (Banyu Pharmaceuticals Co, Tokyo, Japan) was diluted in 100 mL of 0.9%

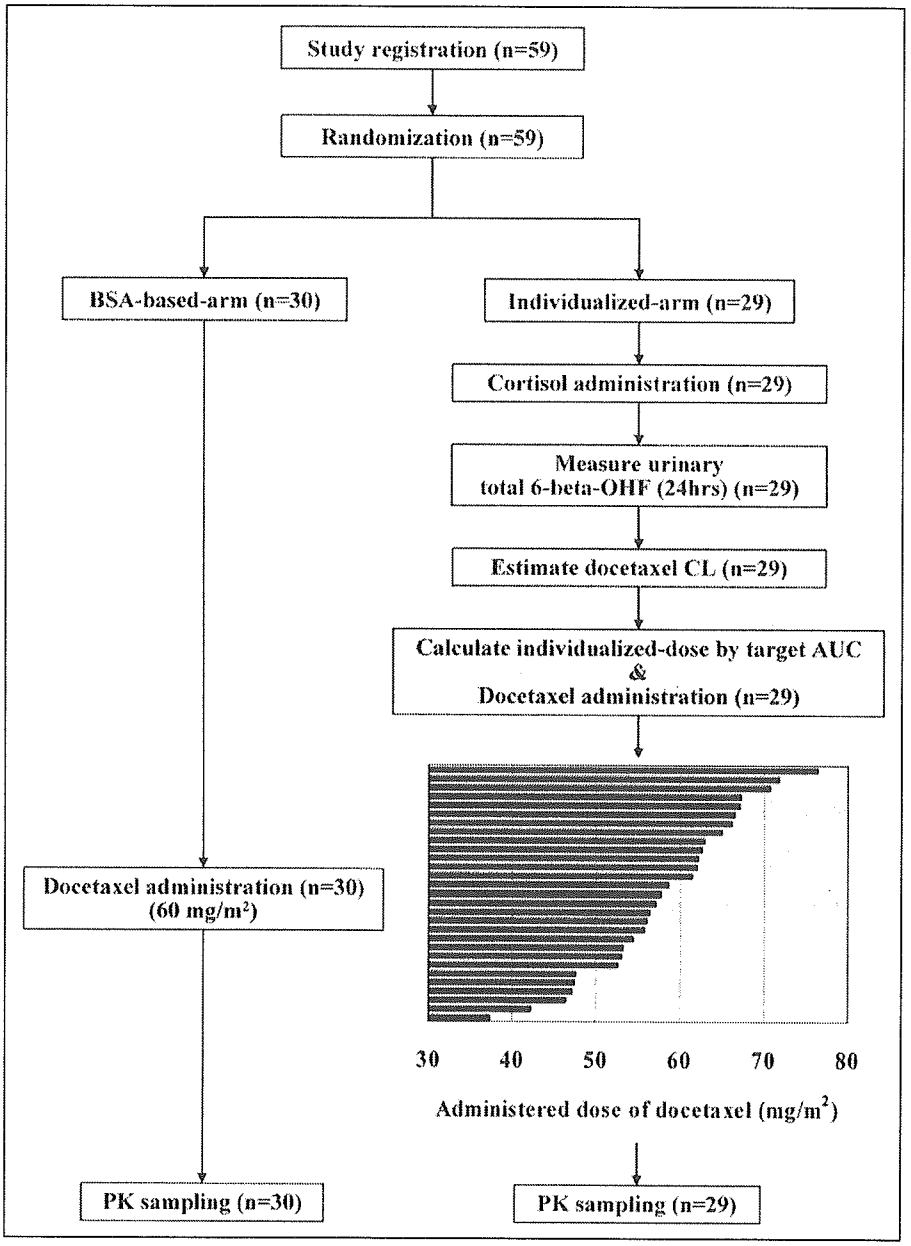

Fig 1. Study flow diagram and administered dose of docetaxel. PK, pharmacokinetic; AUC, area under the concentration-time curve; CL, clearance; 6-β-OHF, 6-beta-hydroxycortisol.

saline and administered intravenously for 30 minutes at 9 AM on day 1 in all patients to estimate the interpatient variability of CYP3A4 activity. After cortisol administration, the urine was collected for 24 hours. The total volume of the 24-hour collection was recorded, and a 5-mL aliquot was analyzed immediately.

Docetaxel Administration

Docetaxel (Taxotere; Aventis Pharm Ltd, Tokyo, Japan) was obtained commercially as a concentrated sterile solution containing 80 mg of the drug in 2 mL of polysorbate 80. In the BSA-based arm, a dose of 60 mg/m^2 of docetaxel was diluted in 250 mL of 5% glucose or 0.9% saline and administered by 1-hour intravenous infusion at 9 AM to all patients.

In the individualized arm, individualized dose of docetaxel was calculated from the estimated CL and the target AUC of 2.66 mg/L · h using the following equations:

$$\text{Estimated CL (L/h/m}^2) = 31.177 + (7.655 \times 10^{-4} \times \text{total-6-}\beta\text{-OHF [}\mu\text{g/d]}) - (4.02 \times \text{AAG [g/L]}) - (0.172 \times \text{AST [U/L]}) - (0.125 \times \text{age [years]})^{30}$$

$$\text{Individualized dose of docetaxel (mg/m}^2) = \text{estimated docetaxel CL (L/h/m}^2) \times \text{target AUC (2.66 mg/L} \cdot \text{h)}$$

At least 2 days after cortisol administration, individualized doses of docetaxel were diluted in 250 mL of 5% glucose or 0.9% saline and administered by 1-hour intravenous infusion at 9 AM to each patient. The doses of docetaxel in subsequent cycles of treatment were unchanged, and no prophylactic premedication to protect against docetaxel-related hypersensitivity reactions was administered in either of the treatment arms.

PK Study

Blood samples for PK studies were obtained from all of the patients during the initial treatment cycle. An indwelling cannula was inserted in the arm opposite that used for the drug infusion, and blood samples were collected into heparinized tubes. Blood samples were collected before the infusion; 30 minutes after the start of the infusion; at the end of the infusion; and 15, 30, and 60 minutes and 3, 5, 9, and 24 hours after the end of the infusion. All blood samples were centrifuged immediately at 4,000 rpm for 10 minutes, after which the plasma was removed and the samples were placed in polypropylene tubes, labeled, and stored at −20°C or colder until analysis.

PK parameters were estimated by the nonlinear least squares regression analysis method (WinNonlin, Version 1.5; Bellkey Science Inc, Chiba, Japan) with a weighting factor of 1 per year.[2] Individual plasma concentration-time data were fitted to two- and three-compartment PK models using a zero-order infusion input and first-order elimination. The model was chosen on the basis of Akaike's information criteria.[31] The peak plasma concentration (C_{max}) was generated directly from the experimental data. AUC was extrapolated to infinity and determined based on the best-fitted curve; this measurement was then used to calculate the absolute CL (L/h), defined as the ratio of the delivered dosage (in milligrams) and AUC.

To assess PD effect of docetaxel, the percentage decrease in ANC was calculated according to the following formula: % decrease in ANC = (pretreatment ANC − nadir ANC)/(pretreatment ANC) × 100.

Measurements

The concentration of urinary 6-β-OHF was measured by reversed phase high-performance liquid chromatography with UV absorbance detection according to previously published methods.[30,32,33]

Docetaxel concentrations in plasma were also measured by solid-phase extraction and reversed phase high-performance liquid chromatography with UV detection according to the previously published method.[30,34] The detection limit corresponded to a concentration of 10 ng/mL.

Statistical Analysis

Fisher's exact test or χ^2 test was used to compare categoric data, and Student's t test was used for continuous variables. The strength of the relationship between the estimated docetaxel CL and the observed docetaxel CL was assessed by least squares linear regression analysis. The interpatient variability of AUC for each arm was evaluated by determining the SD and was compared by F test. Biases, or the mean AUC value in each arm minus the target AUC (2.66 mg/L · h), were also compared between the arms by Student's t test.

A two-sided P value of ≤ .05 or less was considered to indicate statistical significance. All statistical analyses were performed using SAS software version 8.02 (SAS Institute, Cary, NC).

RESULTS

Patient Characteristics

Between October 1999 and May 2001, 59 patients were enrolled onto the study and randomly assigned to either the BSA-based arm (n = 30) or the individualized arm (n = 29). All 59 patients were assessable for PK and PD analyses. The pretreatment characteristics of the 59 patients are listed in Table 1. The baseline characteristics were well balanced between the arms except for three laboratory parameters: ALB, AAG, and ALP. These three parameters were not included in the eligibility criteria. The majority of patients (95%) had a performance status of 0 or 1. Twenty (67%) and 16 (55%) patients had been treated with platinum-based chemotherapy in the BSA-based arm and individualized arm, respectively. Only two patients in the individualized arm had liver metastasis, and most of the patients had good hepatic functions.

Individualized Dosing of Docetaxel

In the individualized arm, the total amount of 24-hour urinary 6-β-OHF after cortisol administration (total 6-β-OHF) was 9,179.6 ± 3,057.7 μg/d (mean ± SD), which was similar to the result of our previous study.[30] The estimated docetaxel CL was 21.9 ± 3.5 L/h/m^2 (mean ± SD), and individualized dose of docetaxel ranged from 37.4 to 76.4 mg/m^2 (mean, 58.1 mg/m^2; Fig 1).

PK

Docetaxel PK data were obtained from all 59 patients during the first cycle of therapy, and PK parameters are listed in Table 2. Drug levels declined rapidly after infusion and could be determined to a maximum of 25 hours. The concentration of docetaxel in plasma was fitted to a biexponential equation, which was consistent with previous reports.[30,35-38] The mean alpha and beta half-lives were 9.2 minutes and 5.0 hours in the BSA-based arm and 9.2 minutes and 7.4 hours in the individualized arm, respectively.

In the BSA-based arm, docetaxel CL was 22.6 ± 3.4 L/h/m^2 (mean ± SD), and AUC averaged 2.71 mg/L · h (range, 2.02 to 3.40 mg/L · h). In the individualized arm, docetaxel CL was 22.1 ± 3.4 L/h/m^2, and AUC averaged 2.64 mg/L · h (range, 2.15 to 3.07 mg/L · h). The least squares linear regression analysis showed that the observed docetaxel CL was well estimated in the individualized arm (r^2 = 0.821; Fig 2).

The SDs of AUC in the BSA-based arm and in the individualized arm were 0.40 and 0.22, respectively, and the ratio of SD in the individualized arm to that in the BSA-based arm was 0.538 (95% CI, 0.369 to 0.782). The biases from the target AUC in the BSA-based arm and in the individualized arm were 0.047 (95% CI, −0.104 to 0.198) and −0.019 (95% CI, −0.102 to 0.064), respectively, with no significant difference. The interpatient variability of

Table 1. Patient Characteristics

Characteristic	BSA-Based Arm No. of Patients	%	Individualized Arm No. of Patients	%	P
Enrolled	30		29		
Eligible	30	100	29	100	
Age, years					.62
Median	61		62		
Range	52-73		45-73		
Sex					
Male	25	83	19	66	.14
Female	5	17	10	34	
ECOG PS					
0	7	23	1	3	.08
1	22	73	26	90	
2	1	3	2	7	
Prior treatment					
None	4	13	4	14	.99
Surgery	11	37	9	31	.65
Radiotherapy	13	43	10	34	.49
Chemotherapy	21	70	18	62	.52
Platinum-based regimens	20	67	16	55	.37
Site of disease					
Lung	23	77	28	97	.10
Liver	0	0	2	7	.24
Pleura	8	27	12	41	.23
Bone	7	23	9	31	.71
Extrathoracic lymph nodes	0	33	10	34	.93
Laboratory parameters					
ALB, g/L					.02
Median	38		35		
Range	26-45		24-44		
AAG, g/L					.04
Median	1.00		1.25		
Range	0.28-2.15		0.64-2.54		
AST, U/L					.67
Median	21		22		
Range	10-40		7-41		
ALT, U/L					.88
Median	18		18		
Range	6-54		4-45		
ALP, U/L					.03
Median	249		324		
Range	129-540		185-986		

Abbreviations: ECOG, Eastern Cooperative Oncology Group; PS, performance status, ALB, serum albumin; AAG, alpha-1-acid glycoprotein; ALP, serum alkaline phosphatase.

AUC was significantly smaller in the individualized arm than in the BSA-based arm ($P < .01$; Fig 3).

PD

In both arms, neutropenia was the predominant toxicity related to docetaxel treatment, and 28 of 30 (93%) patients in the BSA-based arm and 25 of 29 (86%) patients in the individualized arm had grade 3 or 4 neutropenia.

Table 2. Docetaxel PK Parameters

Parameters	BSA-Based Arm (n = 30)	Individualized Arm (n = 29)
C_{max}, μg/mL	0.36-2.70	0.99-2.41
$t_{1/2}$ alpha*, minutes	9.2 ± 3.3	9.2 ± 2.7
$t_{1/2}$ beta*, hours	5.0 ± 4.8	7.4 ± 11.7
CL* L/h	37.6 ± 6.3	34.8 ± 7.1
CL* L/h/m²	22.6 ± 3.4	22.1 ± 3.4
AUC		
Mean mg/L · h	2.71	2.64
Range mg/L · h	2.02-3.40	2.15-3.07
Median	2.65	2.66
SD	0.40	0.22

Abbreviations: PK, pharmacokinetic; BSA, body-surface area; CL, clearance; AUC, area under concentration-time curve; SD, standard deviation.
*Data represent mean ± SD.

Nonhematologic toxicities, such as gastrointestinal and hepatic toxicities (ie, hyperbilirubinemia, aminotransferase elevations), were mild in both arms.

PD effects shown as the percentage decrease in ANC are listed in Table 3. The percentage decrease in ANC for the BSA-based arm and individualized arm were 87.1% (range, 59.0 to 97.7%; SD, 8.7) and 87.5% (range, 78.0 to 97.2%; SD, 6.1), respectively, suggesting that the interpatient variability in the percentage decrease in ANC was slightly smaller in the individualized arm than in the BSA-based arm (Fig 4). The response rates between the two arms were similar; five of 30 (16.7%) and four of 29 (13.8%) patients

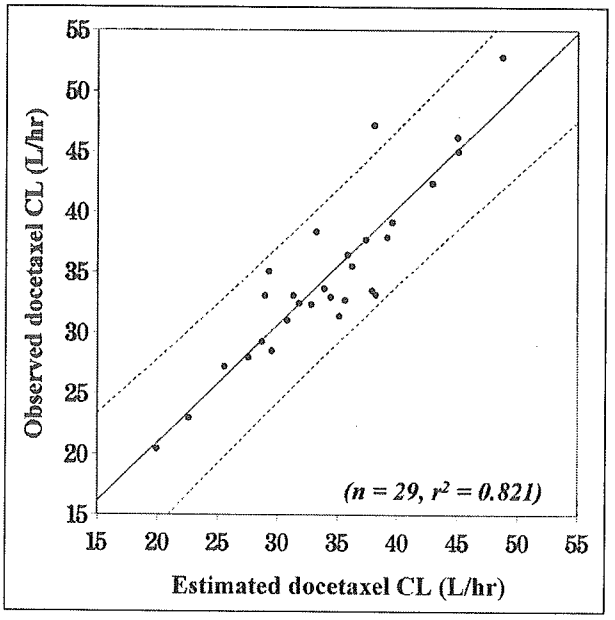

Fig 2. Correlation between the estimated and observed docetaxel clearance (CL) in the individualized arm (n = 29). (—) Linear regression line (r^2 = 0.821); (– – –) 95% CIs for individual estimates.

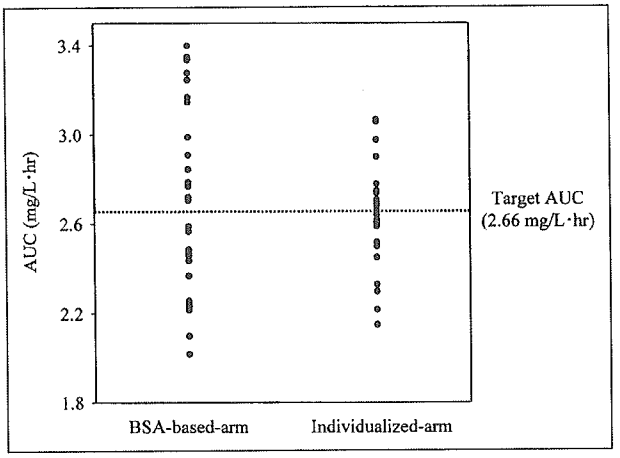

Fig 3. Comparison of area under the concentration-time curve (AUC) variability between the arms ($P < .01$; F test). BSA, body-surface area.

achieved a partial response in the BSA-based arm and individualized arm, respectively.

DISCUSSION

In oncology practice, the prescribed dose of most anticancer drugs is currently calculated from BSA of individual patients to reduce the interpatient variability of drug exposure. However, PK parameters, such as CL of many anticancer drugs, are not related to BSA.[2,39-43] Although PK parameters of docetaxel are correlated with BSA, individualized dosing based on individual metabolic capacities could further decrease the interpatient variability.[43]

CYP3A4 plays an important role in the metabolism of many drugs, including anticancer agents such as docetaxel, paclitaxel, vinorelbine, and gefitinib. This enzyme exhibits a large interpatient variability in metabolic activity, accounting for the large interpatient PK and PD variability. We have developed a novel method of estimating the interpatient variability of CYP3A4 activity by urinary metabolite of exogenous cortisol. That is, the total amount of 24-hour urinary 6-β-OHF after cortisol administration was highly correlated with docetaxel CL. We conducted a prospective randomized PK and PD study of docetaxel to evaluate whether the application of our method to individualized dosing could decrease PK and PD variability compared with BSA-based dosing.

Table 3. Percentage Decrease in ANC

Parameters	BSA-Based Arm (n = 30)	Individualized Arm (n = 29)
Percentage decrease in ANC, %		
Mean	87.1	87.4
Range	59.0-97.7	78.0-97.2
Median	89.7	88.4
SD	8.7	8.1

Abbreviations: ANC, absolute neutrophil count; BSA, body-surface area; SD, standard deviation.

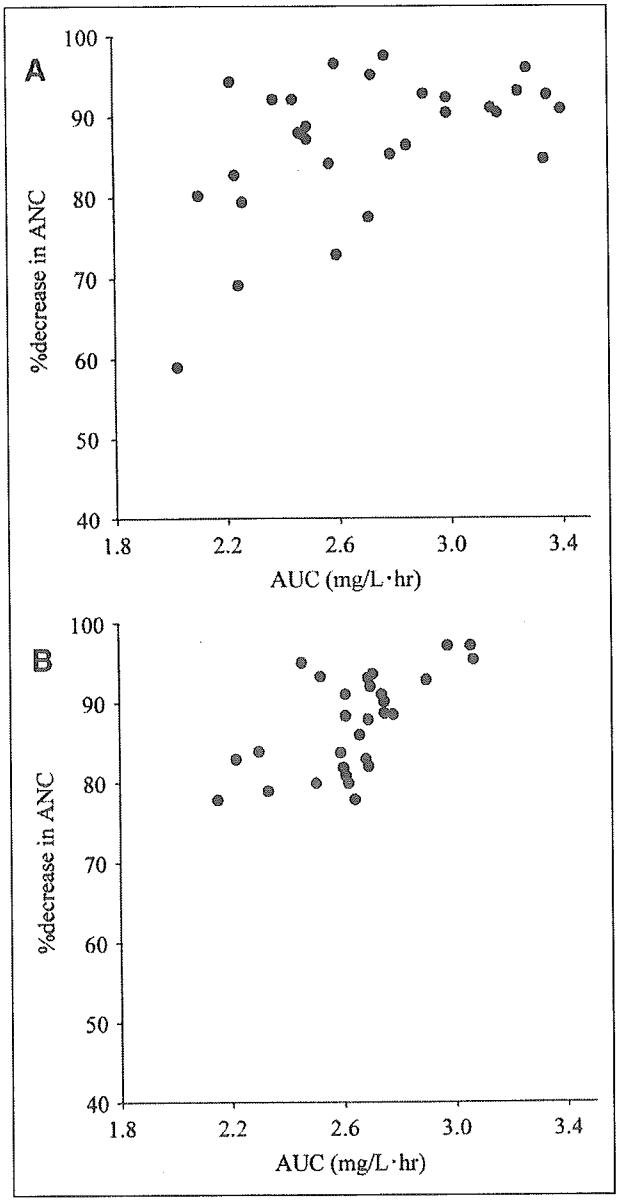

Fig 4. Correlation between area under the concentration-time curve (AUC) and percentage decrease in absolute neutrophil count (ANC) in each arm. (A) body-surface area–based arm; (B) individualized arm.

The study by Hirth et al[28] showed a good correlation between the result of the erythromycin breath test and docetaxel CL, and the study by Goh et al[29] showed a good correlation between the midazolam CL and docetaxel CL. In our study, we prospectively validated the correlation between docetaxel CL and our previously published method using the total amount of urinary 6-β-OHF after

cortisol administration in the individualized arm. As shown in Fig 2, the observed docetaxel CL was well estimated, and the equation for the estimation of docetaxel CL developed in our previous study was found to be reliable and reproducible. The target AUC in the individualized arm was set at 2.66 mg/L · h. This value was the mean value from our previous study, in which 29 patients were treated with 60 mg/m^2 of docetaxel. Individualized doses of docetaxel ranged from 37.4 to 76.4 mg/m^2 and were lower than expected.

The SD of AUC in the individualized arm was about 46.2% smaller than that in the BSA-based arm, a significant difference; this result seems to indicate that the application of our method to individualized dosing can reduce the interpatient PK variability. Assuming that the variability of AUC could be decreased 46.2% by individualized dosing applying our method, overtreatment could be avoided in 14.5% of BSA-dosed patients by using individualized dosing (Fig 5, area A), and undertreatment could be avoided in another 14.5% of these patients (Fig 5, area B). We considered that neutropenia could be decreased with patients in area A by individualized dosing. However, it is unknown whether the therapeutic effect of docetaxel could be improved in the patients in area B by individualized dosing because no significant positive correlation has been found between docetaxel AUC and antitumor response in patients with non–small-cell lung cancer.[43] In this study, seven of 30 (23.3%) and two of 30 (6.7%) patients in the BSA-based arm were included in area A and B, respectively (Figs 3 and 5).

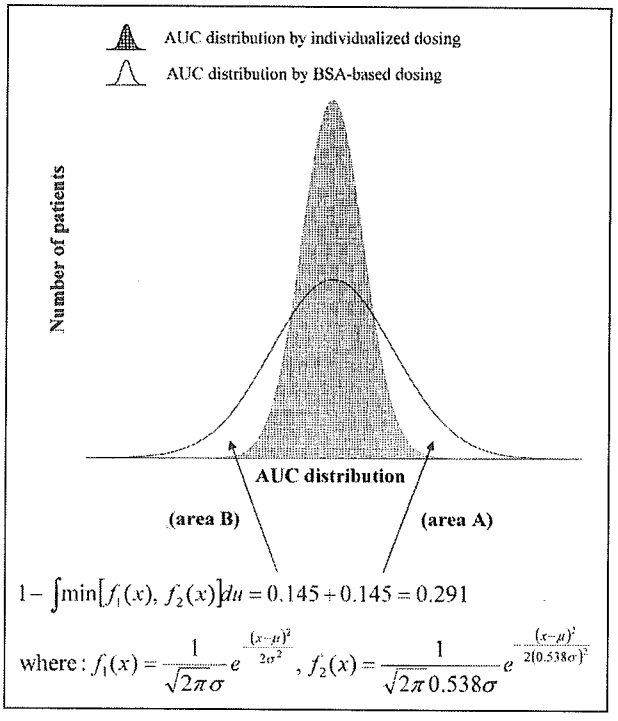

Fig 5. Simulated comparison of area under the concentration-time curve (AUC) distribution between body-surface area (BSA) –based dosing and individualized dosing when the variability of AUC is decreased 46.2% by individualized dosing applied using our method.

As shown in Figure 4, the percentage decrease in ANC was well correlated with AUC in both arms, which was similar to previous reports.[37,43] It was also indicated that the interpatient variability in the percentage decrease in ANC was slightly smaller in the individualized arm than in the BSA-based arm; however, this difference was not significant. The response rates between the two arms were similar. Although the interpatient PK variability could be decreased by individualized dosing in accordance with our method, the interpatient PD variability such as toxicity and the antitumor response could not be decreased. Several reasons could be considered.

With regard to toxicity, the pretreatment characteristics of the patients in this study were highly variable. More than half of the patients in each arm had previously received platinum-based chemotherapy, and more than 30% had received radiotherapy. The laboratory parameters (ie, ALB, AAG, and ALP) were not balanced across the arms, although they were not included in the eligibility criteria (Table 1). These variable pretreatment characteristics and unbalanced laboratory parameters may have influenced the frequency and severity of the hematologic toxicity as well as the pharmacokinetic profiles. The antitumor effect may have been influenced by the intrinsic sensitivity of tumors, the variable pretreatment characteristics, and the imbalance in laboratory parameters. Non–small-cell lung cancer is a chemotherapy-resistant tumor. The response rate for docetaxel ranges from 18% to 38%,[5] and no significant positive correlation between docetaxel AUC and antitumor response has been found. We considered it quite difficult to control the interpatient PD variability by controlling the interpatient PK variability alone. Although we did not observe any outliers in either arm, such as the two outliers with severe toxicity observed in the study by Hirth et al,[28] our method may be more useful for identifying such outliers. If we had not excluded patients with more abnormal liver function or a history of liver disease by the strict eligibility criteria, the results with the two dosing regimens may have been more different, and the interpatient PD variability, such as the percentage decrease in ANC, may have been smaller in the individualized arm than in the BSA-based arm. Furthermore, the primary end point of this study was PK variability, evaluated by the SD of AUC in both arms, and the sample size was significantly underpowered to evaluate whether the application of our method to individualized dosing could decrease PD variability compared with BSA-based dosing.

For the genotypes of CYP3A4, several genetic polymorphisms have been reported (http://www.imm.ki.se/CYPalleles/); however, a clear relationship between genetic polymorphisms and the enzyme activity of CYP3A4 has not been reported. Our phenotype-based

individualized dosing using the total amount of urinary 6-β-OHF after cortisol administration produced good results. However, this method is somewhat complicated, and a simpler method would be of great use. We analyzed the expression of CYP3A4 mRNA in the peripheral-blood mononuclear cells of the 29 patients in the individualized arm. No correlation was observed between the expression level of CYP3A4 mRNA and docetaxel CL or the total amount of urinary 6-β-OHF after cortisol administration (data not shown).

In conclusion, the individualized dosing of docetaxel using the total amount of urinary 6-β-OHF after cortisol administration is useful for decreasing the interpatient PK variability compared with the conventional BSA-based method of dosing. This method may be useful for individualized chemotherapy.

Authors' Disclosures of Potential Conflicts of Interest

The authors indicated no potential conflicts of interest.

REFERENCES

1. Sawyer M, Ratain MJ: Body surface area as a determinant of pharmacokinetics and drug dosing. Invest New Drugs 19:171-177, 2001
2. Gurney H: Dose calculation of anticancer drugs: A review of the current practice and introduction of an alternative. J Clin Oncol 14: 2590-2611, 1996
3. Ratain MJ: Body-surface area as a basis for dosing of anticancer agents: Science, myth, or habit? J Clin Oncol 16:2297-2298, 1998
4. Ringel I, Horwitz SB: Studies with RP 56976 (Taxotere): A semisynthetic analogue of taxol. J Natl Cancer Inst 83:288-291, 1991
5. Cortes JE, Pazdur R: Docetaxel. J Clin Oncol 13:2643-2655, 1995
6. Fossella FV, Lee JS, Murphy WK, et al: Phase II study of docetaxel for recurrent or metastatic non-small-cell lung cancer. J Clin Oncol 12:1238-1244, 1994
7. Fossella FV, Lee JS, Shin DM, et al: Phase II study of docetaxel for advanced or metastatic platinum-refractory non-small-cell lung cancer. J Clin Oncol 13:645-651, 1995
8. Gandara DR, Vokes E, Green M, et al: Activity of docetaxel in platinum-treated non-small-cell lung cancer: Results of a phase II multicenter trial. J Clin Oncol 18:131-135, 2000
9. Kunitoh H, Watanabe K, Onoshi T, et al: Phase II trial of docetaxel in previously untreated advanced non-small-cell lung cancer: A Japanese cooperative study. J Clin Oncol 14:1649-1655, 1996
10. Fossella FV, DeVore R, Kerr RN, et al: Randomized phase III trial of docetaxel versus vinorelbine or ifosfamide in patients with advanced non-small-cell lung cancer previously treated with platinum-containing chemotherapy regimens: The TAX 320 Non-Small Cell Lung Cancer Study Group. J Clin Oncol 18:2354-2362, 2000
11. Shepherd FA, Dancey J, Ramlau R, et al: Prospective randomized trial of docetaxel versus best supportive care in patients with non–small-cell lung cancer previously treated with platinum-based chemotherapy. J Clin Oncol 18:2095-2103, 2000
12. Hudis CA, Seidman AD, Crown JP, et al: Phase II and pharmacologic study of docetaxel as initial chemotherapy for metastatic breast cancer. J Clin Oncol 14:58-65, 1996
13. Trudeau ME, Eisenhauer EA, Higgins BP, et al: Docetaxel in patients with metastatic breast cancer: A phase II study of the National Cancer Institute of Canada-Clinical Trials Group. J Clin Oncol 14:422-428, 1996
14. Chan S, Friedrichs K, Noel D, et al: Prospective randomized trial of docetaxel versus doxorubicin in patients with metastatic breast cancer: The 303 Study Group. J Clin Oncol 17:2341-2354, 1999
15. Marre F, Sanderink GJ, de Sousa G, et al: Hepatic biotransformation of docetaxel (Taxotere) *in vitro*: Involvement of the CYP3A subfamily in humans. Cancer Res 56:1296-1302, 1996
16. Nelson DR, Koymans L, Kamataki T, et al: P450 superfamily: Update on new sequences, gene mapping, accession numbers and nomenclature. Pharmacogenetics 6:1-42, 1996
17. Lin JH, Lu AYH: Inhibition and induction of cytochrome P450 and the clinical implications. Clin Pharmacokinet 35:361-390, 1998
18. Parkinson A: An overview of current cytochrome P450 technology for assessing the safety and efficacy of new materials. Toxicol Pathol 24:45-57, 1996
19. Shimada T, Yamazaki H, Mimura M, et al: Interindividual variations in human liver cytochrome P-450 enzymes involved in the oxidation of drugs, carcinogens and toxic chemicals: Studies with liver microsomes of 30 Japanese and 30 Caucasians. J Pharmacol Exp Ther 270:414-423, 1994
20. Guengerich FP: Characterization of human microsomal cytochrome P450 enzymes. Annu Rev Pharmacol Toxicol 29:241-264, 1989
21. Guengerich FP, Turvy CG: Comparison of levels of human microsomal cytochrome P450 enzymes and epoxide hydrolase in normal and disease status using immunochemical analysis of surgical samples. J Pharmacol Exp Ther 256: 1189-1194, 1991
22. Hunt CM, Westerkam WR, Stave GM: Effects of age and gender on the activity of human hepatic CYP3A. Biochem Pharmacol 44: 275-283, 1992
23. Watkins PB, Turgeon DK, Saenger P, et al: Comparison of urinary 6-beta-cortisol and the erythromycin breath test as measures of hepatic P450IIIA (CYP3A) activity. Clin Pharmacol Ther 52:265-273, 1992
24. Kinirons MT, O'Shea D, Downing TE, et al: Absence of correlations among three putative *in vivo* probes of human cytochrome P4503A activity in young healthy men. Clin Pharmacol Ther 54:621-629, 1993
25. Hunt CM, Watkins PB, Saenger P, et al: Heterogeneity of CYP3A isoforms metabolizing erythromycin and cortisol. Clin Pharmacol Ther 51:18-23, 1992
26. Thummel KE, Shen DD, Podoll TD, et al: Use of midazolam as a human cytochrome P450 3A probe: II. Characterization of inter- and intra-individual hepatic CYP3A variability after liver transplantation. J Pharmacol Exp Ther 271:557-566, 1994
27. Thummel KE, Shen DD, Podoll TD, et al: Use of midazolam as a human cytochrome P450 3A probe: I. In vitro-in vivo correlations in liver transplant patients. J Pharmacol Exp Ther 271: 549-556, 1994
28. Hirth J, Watkins PB, Strawderman M, et al: The effect of an individual's cytochrome CYP3A4 activity on docetaxel clearance. Clin Cancer Res 6:1255-1258, 2000
29. Goh BC, Lee SC, Wang LZ, et al: Explaining interindividual variability of docetaxel pharmacokinetics and pharmacodynamics in Asians through phenotyping and genotyping strategies. J Clin Oncol 20:3683-3690, 2002
30. Yamamoto N, Tamura T, Kamiya Y, et al: Correlation between docetaxel clearance and estimated cytochrome P450 activity by urinary metabolite of exogenous cortisol. J Clin Oncol 18:2301-2308, 2000
31. Yamaoka K, Nakagawa T, Uno T: Application of Akaike's information criterion (AIC) in the evaluation of linear pharmacokinetic equations. J Pharmacokinet Biopharm 6:165-175, 1978
32. Nakamura J, Yakata M: Determination of urinary cortisol and 6 beta-hydroxycortisol by high performance liquid chromatography. Clin Chim Acta 149:215-224, 1985
33. Lykkesfeldt J, Loft S, Poulsen HE: Simultaneous determination of urinary free cortisol and 6 beta-hydroxycortisol by high-performance liquid chromatography to measure human CYP3A activity. J Chromatogr B Biomed Appl 660:23-29, 1994
34. Vergniol JC, Bruno R, Montay G, et al: Determination of Taxotere in human plasma by a semi-automated high-performance liquid chromatographic method. J Chromatogr 582:273-278, 1992
35. Taguchi T, Furue H, Niitani H, et al: Phase I clinical trial of RP 56976 (docetaxel) a new anticancer drug. Gan To Kagaku Ryoho 21:1997-2005, 1994
36. Burris H, Irvin R, Kuhn J, et al: Phase I clinical trial of Taxotere administered as either a 2-hour or 6-hour intravenous infusion. J Clin Oncol 11:950-958, 1993
37. Extra JM, Rousseau F, Bruno R, et al: Phase I and pharmacokinetic study of Taxotere (RP 56976; NSC 628503) given as a short

intravenous infusion. Cancer Res 53:1037-1042, 1993

38. Pazdur R, Newman RA, Newman BM, et al: Phase I trial of Taxotere: Five-day schedule. J Natl Cancer Inst 84:1781-1788, 1992

39. Mathijssen RHJ, Verweij J, de Jonge MJ, et al: Impact of body-size measures on irinotecan clearance: Alternative dosing recommendations. J Clin Oncol 20:81-87, 2002

40. De Jongh FE, Verweij J, Loos WJ, et al: Body-surface area-based dosing does not increase accuracy of predicting cisplatin exposure. J Clin Oncol 19:3733-3739, 2001

41. Gurney HP, Ackland S, Gebski V, et al: Factors affecting epirubicin pharmacokinetics and toxicity: Evidence against using body-surface area for dose calculation. J Clin Oncol 16:2299-2304, 1998

42. Loos WJ, Gelderblom H, Sparreboom A, et al: Inter- and intrapatient variability in oral topotecan pharmacokinetics: Implications for body-surface area dosage regimens. Clin Cancer Res 6:2685-2689, 2000

43. Bruno R, Hille D, Riva A, et al: Population pharmacokinetics/pharmacodynamics of docetaxel in phase II studies in patients with cancer. J Clin Oncol 16:187-196, 1998

Lung Cancer (2005) 49, 217–223

ELSEVIER

LUNG CANCER

IASLC

www.elsevier.com/locate/lungcan

Clinical responses of large cell neuroendocrine carcinoma of the lung to cisplatin-based chemotherapy

Shigeo Yamazaki[a,d], Ikuo Sekine[a,*], Yoshihiro Matsuno[b], Hidefumi Takei[c], Noboru Yamamoto[a], Hideo Kunitoh[a], Yuichiro Ohe[a], Tomohide Tamura[a], Tetsuro Kodama[a], Hisao Asamura[c], Ryosuke Tsuchiya[c], Nagahiro Saijo[a]

[a] *Division of Thoracic Oncology and Internal Medicine, National Cancer Center Hospital, Tsukiji 5-1-1, Chuo-ku, Tokyo 104-0045, Japan*
[b] *Division of Clinical Laboratory, National Cancer Center Hospital, Tokyo*
[c] *Division of Thoracic Surgery, National Cancer Center Hospital, Tokyo*
[d] *Department of Surgery, Keiyu-kai Sapporo Hospital, Sapporo, Japan*

Received 30 September 2004; received in revised form 3 January 2005; accepted 3 January 2005

KEYWORDS
Neuroendocrine carcinoma;
Lung cancer;
Chemotherapy;
Cisplatin

Summary
Background: The efficacy of chemotherapy in patients with large cell neuroendocrine carcinoma of the lung (LCNEC) remains unclear.
Methods: Patients with LCNEC who received cisplatin-based chemotherapy were identified by reviewing 567 autopsied and 2790 surgically resected lung cancer patients. The clinical characteristics and objective responses to chemotherapy in these patients were analyzed.
Results: Overall, 20 cases of LCNEC were identified, including stage IIIA ($n=3$), stage IIIB ($n=6$), stage IV ($n=6$) and postoperative recurrence ($n=5$) cases. Six patients had received prior chemotherapy, and 14 were chemo-naive patients. The patients had received a combination of cisplatin and etoposide ($n=9$), cisplatin, vindesine and mitomycin ($n=6$), cisplatin and vindesine ($n=4$), or cisplatin alone ($n=1$). One patient showed complete response and nine showed partial response, yielding an objective response rate of 50%. The response rate did not differ between patients with the initial diagnosis of SCLC and those with the initial diagnosis of NSCLC, however, the response rate in chemo-naive patients (64%) was significantly different from that in previously treated patients (17%).
Conclusions: Our results suggest that the response rate of LCNEC to cisplatin-based chemotherapy was comparable to that of SCLC.

* Corresponding author. Tel.: +81 3 3542 2511; fax: +81 3 3542 3815.
E-mail address: isekine@ncc.go.jp (I. Sekine).

0169-5002/$ – see front matter © 2005 Elsevier Ireland Ltd. All rights reserved.
doi:10.1016/j.lungcan.2005.01.008

1. Introduction

Pulmonary neuroendocrine tumors include a spectrum of four clinicopathological entities classified on the basis of the morphological and biological features: typical carcionoid and atypical carcinoid, which are tumors of low to intermediate grade malignancy, and large cell neuroendocrine carcinoma (LCNEC) and small cell carcinoma (SCLC), which are high-grade malignant tumors. Travis et al. proposed the term LCNEC in 1991 [1], for classifying a type of poorly differentiated high-grade carcinoma characterized by a neuroendocrine appearance under light microscopy. LCNEC exhibits more prominent cellular pleomorphism and higher mitotic activity than the atypical carcinoid (AC), and is distinguished from SCLC by the tumor cell size and chromatin morphology. Although several different terminologies and classifications have been proposed previously, and even the present classification of pulmonary neuroendocrine tumors lacks uniform definition criteria, this class of tumors could become widely accepted and included in the updated histological classification of the World Health Organization [2].

The clinical features of LCNEC have not yet been completely clarified. The prognosis of patients with surgically resected LCNEC is reported to be intermediate between that of AC and SCLC [3–5], and the same as that of resected NSCLC, except that stage I LCNEC has a poorer prognosis than stage I non-small cell lung cancer (NSCLC) [6]. To the best of our knowledge, however, there are no studies that have examined the role of chemotherapy for LCNEC and the prognosis of patients with unresectable LCNEC, even though several reports have been published on the association between response to chemotherapy and the neuroendocrine differentiation of NSCLC [7–9]. The appropriate treatment of unresectable LCNEC, therefore, remains unclear. In the present study, we attempted to investigate the effectiveness of chemotherapy with cisplatin-based regimens for LCNEC in patients with unresectable and recurrent LCNEC.

2. Materials and methods

Eighty-seven of 2790 patients with primary lung cancer who underwent tumor resection from 1982 to 1999 at the National Cancer Center Hospital were found to have tumors with the histological characteristics of LCNEC [6]. Of these, five had received cisplatin-based chemotherapy at the time of recurrence, and were enrolled as subjects of this study. In addition, 303 of 567 patients who were autopsied from 1983 to 1997 at the National Cancer Center Hospital who had the following histological diagnoses were first selected: SCLC ($n=112$), poorly differentiated adenocarcinoma ($n=99$), large cell carcinoma ($n=58$), poorly differentiated squamous cell carcinoma ($n=29$), poorly differentiated adenosquamous carcinoma ($n=2$), LCNEC ($n=2$), and carcinoid ($n=1$). Of these, 161 had received cisplatin-based chemotherapy were selected for a pathological review. Finally, specimens from 17 of these161 cases were found to have histological characteristics consistent with the diagnosis of LCNEC, and were selected as subjects of this study. We focused on cisplatin, because since the 1980s, cisplatin has been the only anticancer agent with proven efficacy against both SCLC and NSCLC [10,11]; we, therefore, considered that the effectiveness of chemotherapy for LCNEC could be reasonably evaluated if cisplatin were included in the regimen. Cases which had received adjuvant chemotherapy without evaluable lesions were excluded from the analysis.

All the available paraffin-embedded tissue sections stained with hematoxylin–eosin were reviewed. We classified LCNEC according to the histopathological criteria in the WHO classification [2]. Immunohistochemical analysis was performed to confirm the neuroendocrine features of the tumors. For this purpose, formalin-fixed paraffin sections were stained for a panel of neuroendocrine markers, including chromogranin A (CGA), synaptophysin (SYN), and neural cell adhesion molecule (NCAM), using standard methods. The intensity of immunostaining for these markers was scored as follows: +, when the proportion of stained tumor cells was >50%; ±, when 10–50% of tumor cells were stained; and −, when <10% of tumor cells were stained, as previously described [6]. One case included in this study had the typical histological features of LCNEC, but no neuroendocrine features as determined by the immunohistochemical analysis. For specimens obtained after treatment, we routinely confirmed that the histopathological and morphological features showed no changes due to treatment as compared with the pretreatment biopsy or cytologic specimens. Such cases for which no pretreatment samples were available were excluded from the study; since it has been reported that histological changes may occur after treatment in SCLC [12], we were concerned that misdiagnosis might occur if the same were also true for LCNEC.

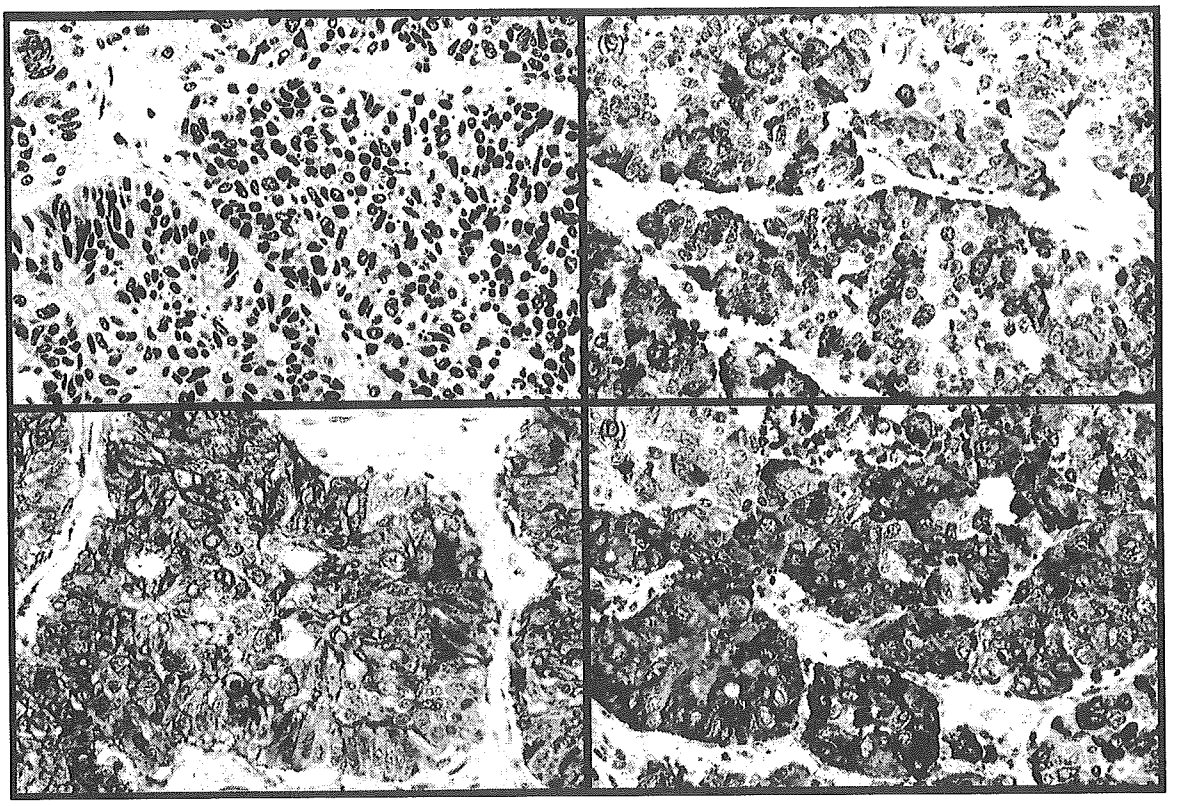

Fig. 1 Case no. 2, 57-year-old man. (A) The tumor cells which are large-sized, polygonal in shape and have a low nuclear-cytoplasmic ratio, are arranged in organoid nests and trabeculae (H&E stain, ×200). Positive staining for neural cell adhesion molecule (B), chromogranin A (C), and synaptophysin (D) (immunostain, ×400).

Clinical information about the cases was obtained from the medical records. The clinical disease staging was reassessed according to the latest International Union Against Cancer (UICC) staging criteria [13]. The response to chemotherapy and overall survival rate were assessed retrospectively. The objective tumor response was evaluated according to the WHO criteria published in 1979 (WHO, 1979) [14]. The survival time was measured from the date of start of chemotherapy with a cisplatin-containing regimen. Survival curves were drawn using the Kaplan–Meier method [15]. Drug toxicity could not be assessed as the study was a retrospective one and records were often incomplete.

3. Results

Overall, 22 cases were recognized as having tumors with histological characteristics consistent with LCNEC among the autopsied and surgically resected cases of primary lung cancer that had received cisplatin-based chemotherapy and had evaluable lesions; of these 17 were autopsied cases and five were surgically resected cases. Two of the autopsied cases were excluded, because no pretreatment pathological or cytological samples were available. The typical microscopic appearance of the tumor specimens is shown in Fig. 1A. The specimen sources for the prechemotherapy-diagnosis included surgically resected specimens ($n = 5$), biopsy specimens ($n = 9$), and cytology specimens ($n = 6$). The histological and cytological findings in the specimens obtained before chemotherapy were consistent with those in the specimens obtained after chemotherapy. We therefore finally enrolled 20 cases in this study. The initial pathologic diagnoses in these patients were as follows: small cell carcinoma ($n = 10$), poorly differentiated adenocarcinoma ($n = 6$), large cell carcinoma ($n = 2$), undifferentiated carcinoma ($n = 1$), and poorly differentiated carcinoma ($n = 1$) (Table 1). None of the cases had been labeled as LCNEC at the time of initial diagnosis, probably because the concept of LCNEC

Table 1 Patient characteristics

Characteristics	N	%
No. of patients	20	
Sex		
Male	18	90
Female	2	10
Age, median (range)	58 (37–74)	
Smoking history		
Yes	19	95
No	1	5
Performance status		
1–2	19	95
>2	1	5
Initial pathological diagnosis		
Small cell carcinoma	10	50
Adenocarcinoma	6	30
Large cell carcinoma	2	10
Others	2	10
Clinical stage at the start of chemotherapy		
IIIA	3	15
IIIB	6	30
IV	6	30
Postoperative recurrence	5	25
Prior treatment		
None	10	50
Surgery	4	20
Radiotherapy	2	10
Chemotherapy without cisplatin	6	30

Table 2 Staining for neuroendocrine markers in 20 LCNECs

Case	NCAM	CGA	SYN
1	+	+	+
2	+	+	+
3	+	+	+
4	±	+	+
5	+	+	+
6	+	+	+
7	−	+	−
8	+	−	−
9	−	−	−
10	−	+	±
11	+	−	+
12	+	+	+
13	+	+	+
14	+	−	±
15	+	+	+
16	+	−	NA
17	+	−	+
18	+	−	NA
19	+	−	+
20	−	+	+

NCAM, neural cell adhesion molecule; CGA, chromogranin A; SYN, synaptophysin; NA, not assessed.

was not completely accepted at our hospital at that time.

The results of the immunohistochemical staining are shown in Table 2, and a typical case showing positive staining is shown in Fig. 1B and D. Of the 20 LCNECs, 19 expressed at least one of the three general neuroendocrine markers, namely CGA, SYN, and NCAM. Sixteen of the 20 LCNECs exhibited positive staining for NCAM, while one showed equivocal staining. Twelve of the 20 LCNECs showed positive staining for CGA. Thirteen LCNECs showed positive staining for SYN and three showed equivocal staining. Only one case was negative for all the three general neuroendocrine markers, however, this case exhibited the typical histological features of LCNEC on light microscopy.

The clinical characteristics of the patients are summarized in Table 1. The extremely high predominance of men and smokers in this study was comparable to the demographic features of our LCNEC patients treated by surgical resection [6]. Previous chemotherapy was given in six patients: nedaplatin in one and cyclophosphamide-based regimen in five patients. The chemotherapy regimens used were as follows: cisplatin (80 mg/m^2, day 1) and etoposide (100 mg/m^2, days 1–3) (n = 9), cisplatin (80 mg/m^2, day 1), vindesine (3 mg/m^2, days 1 and 8) and mitomycin (8 mg/m^2, day 1) (n = 6), cisplatin (80 mg/m^2, day 1) and vindesine (3 mg/m^2, days 1 and 8) (n = 4), or cisplatin (100 mg/m^2, day 1) alone (n = 1). The median (range) number chemotherapy cycles were 2 (1–6). Of the 20 patients, one showed CR and nine showed PR, yielding an overall response rate of 50% (95% confidence interval, 27.2–72.8%). One CR and four PRs were observed among the cases treated with cisplatin and etoposide, two PRs were found among those treated with cisplatin, vindesine and mitomycin, and three PRs were found among those treated with cisplatin and vindesine. Seven patients showed NC, and three showed progressive disease. While the response rate did not differ between patients with an initial diagnosis of SCLC and those patients with an initial diagnosis of NSCLC, previous chemotherapy affected the response to cisplatin: the response rate in chemo-naive patients was 64%, whereas that in previously treated patients was 17%. The median progression-free survival in the 20 patients was 103 days, median survival was 239 days, 1-year survival rate was 35%, and 2-year survival rate was 15%.

4. Discussion

In this extensive review of over 3000 lung cancer patients, we found considerable difficulty in evaluating the response of LCNEC to systemic chemotherapy. The pathological diagnosis of LCNEC was established in 87 (3.1%) of 2790 patients treated by surgical resection. This low incidence of LCNEC in surgically treated lung cancer patients is comparable to that in other previously published reports: 2.4% (50/2070), 2.9% (22/766), and 3.6% (53/1530) [16–18]. Of the 87 patients, only five who had received cisplatin-based chemotherapy for recurrent tumor that was evaluable for the response. While LCNEC is difficult to diagnose prior to the start of treatment on the basis of the findings in biopsy or cytological specimens, the architectural neuroendocrine features may, more or less, be reflected in these small samples [19,20]. We, therefore, conducted a review of 567 autopsy cases of lung cancer, and identified 15 cases of LCNEC who had received cisplatin-based chemotherapy. We obtained a response rate to cisplatin-based chemotherapy of 50% in these 20 patients with LCNEC, however, the clinical characteristics of patients with medically treatable advanced LCNEC would still remain to be clarified, because autopsy is conducted only in highly selective cases.

Travis et al. suggested that immunohistochemical or electron-microscopic evidence of neuroendocrine features were important to diagnose LCNEC [1]. We assessed the neuroendocrine marker expression by immunohistochemical staining for CGA, SYN, and NCAM. Our cases included one that was negative for all the three neuroendocrine markers examined, but showed the typical histological features of LCNEC, which could be attributable to technical staining problems. Immunohistochemical staining for neuroendocrine tumors is generally recognized as only a supplementary diagnostic tool. In addition, the post-surgical survival rate did not differ between histologically diagnosed cases of LCNEC with neuroendocrine differentiation in marker expression as assessed by immunohistochemical staining and large cell carcinoma with neuroendocrine morphology where the neuroendocrine markers were negative (data not shown). Thus, we decided to include the case with negative staining as LCNEC on the basis of its typical neuroendocrine morphology.

To the best of our knowledge, only one study on the efficacy of chemotherapy in patients with LCNEC has been reported previously. In the study, 13 patients with LCNEC received chemotherapy when relapse was noted after surgical resection, and two (20%) of 10 evaluable patients showed an objective response. The evaluable lesion in these patients, however, was the brain in seven, liver in two, and bone in one patient [21]. Thus, the relatively low response rate in the report may be due to the site of the evaluable lesion. In addition, reports on the correlation between response to chemotherapy and neuroendocrine differentiation of NSCLC may be helpful. Graziano et al. reported that the proportion of NSCLC positive for neuroendocrine markers was higher in responders than in non-responders among 52 NSCLC patients treated by chemotherapy, and that the result suggested a correlation between positivity for neuroendocrine marker expression and the likelihood of response to chemotherapy [7]. On the other hand, others have reported the absence of any correlation between the presence of neuroendocrine differentiation and the response to chemotherapy [8,9]. The neuroendocrine differentiation in NSCLCs in the aforementioned studies was confirmed only by immunohistochemical staining and not on the basis of the morphological definition of LCNEC. Therefore, these groups might have potentially included heterogeneous subtypes of lung carcinoma, such as adenocarcinoma or squamous cell carcinoma, with components of neuroendocrine differentiation. The conflicting conclusions of these studies may, therefore, reflect differences in the biological characteristics of the tumors included in the analysis. Since the definition of LCNEC is based on morphological criteria as well as positivity for neuroendocrine marker expression, LCNEC is may be considered to be a clinically homogeneous group. Therefore, our study of LCNEC may endorse the former reports about the relationship between neuroendocrine differentiation and the sensitivity to chemotherapy.

Objective response to chemotherapy can be observed in only 15–30% of NSCLCs, even when they are treated with regimens containing cisplatin [10]. In SCLC, however, effective combination regimens yield objective response rates in the range of 80–90% [11]. Our study showed an overall response rate of LCNEC of 50% to cisplatin-based chemotherapy, and a response rate of 64% in chemo-naive patients, which seemed to be higher than the response rate of NSCLC to chemotherapy. Considered together, these results suggest that the chemosensitivity of LCNEC is intermediate between that of NSCLC and SCLC, although we were unable to obtain firm evidence from this retrospective study, which included only a small cohort of patients.

Since LCNEC is a relatively rare subtype of lung cancer, a prospective study is difficult to perform, and may only be possible as a multicenter study.

For this purpose, it is an urgent task to establish diagnostic criteria for LCNEC based on examination of biopsy or cytologic specimens. Although the histological definition of LCNEC in surgically resected specimens proposed by Travis et al. is commonly accepted, its diagnostic reproducibility is not satisfactory [22]. It is also difficult to apply the definition to biopsy specimens, in which artifacts can easily be produced and detailed examination may be difficult due to insufficient specimen size. Thus, definitive diagnostic criteria also applicable to biopsy and cytologic specimens are required.

Our study did not include any cases labeled as LCNEC at the time of initial diagnosis. One half of the cases was originally diagnosed as SCLC and the other half as NSCLC, including poorly differentiated adenocarcinoma and large cell carcinoma. This was attributed to the fact that the concept of LCNEC was not clearly defined prior to its being proposed by Travis et al. [1]. Thus, it is possible that patients with LCNEC were included in earlier clinical trials for NSCLC or SCLC. If LCNEC shares the poor prognosis of NSCLC, the reported results of chemotherapy for NSCLC may have been worse in studies in which cases of LCNEC were included. Similarly, the results of clinical studies of SCLC to study their objective response to chemotherapy may also have been worse because of the confounding effects of the inclusion of LCNECs among the cases.

In conclusion, our results suggest that the response rate of LCNEC to cisplatin-based chemotherapy was comparable to that of SCLC. However, because of the retrospective nature of this study and the small sample size, we could not arrive at any definitive conclusion; we, therefore, propose to conduct a prospective study in the future aimed at elucidating the efficacy of chemotherapy for LCNEC. To that end, firm diagnostic criteria for LCNEC need to be established, even when the diagnosis must be based only on examination of biopsy and cytology specimens.

Acknowledgment

We thank Ms. Yuko Yabe for kindly preparing this manuscript.

References

[1] Travis WD, Linnoila RI, Tsokos MG, Hitchcock CL, Cutler Jr GB, Nieman L, et al. Neuroendocrine tumors of the lung with proposed criteria for large-cell neuroendocrine carcinoma. An ultrastructural, immunohistochemical, and flow cytometric study of 35 cases. Am J Surg Pathol 1991;15:529–53.

[2] Travis W, Corrin B, Shimosato Y, Brambilla E. Histological typing of lung and pleural tumours. Berlin: Springer-Verlag; 1999.

[3] Rusch VW, Klimstra DS, Venkatraman ES. Molecular markers help characterize neuroendocrine lung tumors. Ann Thorac Surg 1996;62:798–809 [discussions 09–10].

[4] Dresler CM, Ritter JH, Patterson GA, Ross E, Bailey MS, Wick MR. Clinical-pathologic analysis of 40 patients with large cell neuroendocrine carcinoma of the lung. Ann Thorac Surg 1997;63:180–5.

[5] Travis WD, Rush W, Flieder DB, Falk R, Fleming MV, Gal AA, et al. Survival analysis of 200 pulmonary neuroendocrine tumors with clarification of criteria for atypical carcinoid and its separation from typical carcinoid. Am J Surg Pathol 1998;22:934–44.

[6] Takei H, Asamura H, Maeshima A, Suzuki K, Kondo H, Niki T, et al. Large cell neuroendocrine carcinoma of the lung: a clinicopathologic study of eighty-seven cases. J Thorac Cardiovasc Surg 2002;124:285–92.

[7] Graziano SL, Mazid R, Newman N, Tatum A, Oler A, Mortimer JA, et al. The use of neuroendocrine immunoperoxidase markers to predict chemotherapy response in patients with non-small-cell lung cancer. J Clin Oncol 1989;7:1398–406.

[8] Schleusener JT, Tazelaar HD, Jung SH, Cha SS, Cera PJ, Myers JL, et al. Neuroendocrine differentiation is an independent prognostic factor in chemotherapy-treated nonsmall cell lung carcinoma. Cancer 1996;77:1284–91.

[9] Carles J, Rosell R, Ariza A, Pellicer I, Sanchez JJ, Fernandez-Vasalo G, et al. Neuroendocrine differentiation as a prognostic factor in non-small cell lung cancer. Lung Cancer 1993;10:209–19.

[10] Ginsberg RJ, Vokes EE, Rosenzweig K. Non-small cell lung cancer. In: DeVita VT, Hellman S, Rosenberg SA, editors. Cancer: principles & practice of oncology. 6th ed. Philadelphia: Lippincott Williams & Wilkins; 2001. p. 925–83.

[11] Murren J, Glatstein E, Pass HI. Small cell lung cancer. In: DeVita VT, Hellman S, Rosenberg SA, editors. Cancer: principles & practice of oncology. 6th ed. Philadelphia: Lippincott Williams & Wilkins; 2001. p. 983–1018.

[12] Fushimi H, Kikui M, Morino H, Yamamoto S, Tateishi R, Wada A, et al. Histologic changes in small cell lung carcinoma after treatment. Cancer 1996;77:278–83.

[13] Sobin LH, Wittenkind C. TNM classification of malignant tumors. New York: Wiley-Liss; 1997.

[14] Handbook for reporting results of cancer treatment. Geneva: World Health Organization (WHO); 1979.

[15] Kaplan ELMP. Non-parametric estimation from incomplete observations. J Am Stat Assoc 1958;53:457–81.

[16] Jiang SX, Kameya T, Shoji M, Dobashi Y, Shinada J, Yoshimura H. Large cell neuroendocrine carcinoma of the lung: a histologic and immunohistochemical study of 22 cases. Am J Surg Pathol 1998;22:526–37.

[17] Iyoda A, Hiroshima K, Toyozaki T, Haga Y, Fujisawa T, Ohwada H. Clinical characterization of pulmonary large cell neuroendocrine carcinoma and large cell carcinoma with neuroendocrine morphology. Cancer 2001;91:1992–2000.

[18] Paci M, Cavazza A, Annessi V, Putrino I, Ferrari G, De Franco S, et al. Large cell neuroendocrine carcinoma of the lung: a 10-year clinicopathologic retrospective study. Ann Thorac Surg 2004;77:1163–7.

[19] Yang YJ, Steele CT, Ou XL, Snyder KP, Kohman LJ. Diagnosis of high-grade pulmonary neuroendocrine carcinoma by fine-needle aspiration biopsy: nonsmall-cell or small-cell type? Diagn Cytopathol 2001;25:292–300.

[20] Wiatrowska BA, Krol J, Zakowski MF. Large-cell neuroendocrine carcinoma of the lung: proposed criteria for cytologic diagnosis. Diagn Cytopathol 2001;24:58–64.
[21] Mazieres J, Daste G, Molinier L, Berjaud J, Dahan M, Delsol M, et al. Large cell neuroendocrine carcinoma of the lung: pathological study and clinical outcome of 18 resected cases. Lung Cancer 2002;37:287–92.
[22] Travis WD, Gal AA, Colby TV, Klimstra DS, Falk R, Koss MN. Reproducibility of neuroendocrine lung tumor classification. Hum Pathol 1998;29:272–9.